IDENTIFICATION OF POTENTIAL MAGL INHIBITORS USING MOLECULAR DOCKING SCREENING AS ANTI-CANCER AGENTS

Abhishek Kashyap [1], Dimpy Rani[1*], Suresh Kumar[1], Rohit Dutt[1]

[1] Department of Pharmaceutical Chemistry, School of Medical and Allied Sciences, G. D. Goenka University, Sohna – 122003, India

Corresponding Author Details:
Dimpy Rani, Department of Pharmaceutical Chemistry, School of Medical and Allied Sciences, G. D.Goenka University, Sohna – 122003, India
Email: dimpy.rani.gdgu@gmail.com

ABSTRACT:

MAGL is an important key enzyme responsible for various factors in the human body and the development of disorders like pain, inflammation, CNS disorders and cancer. MAGL has an important function in the endocannabinoid system and is responsible for of hydrolysis one of the endocannabinoids, 2-arachidononoylglycerol lipase. 2-arachidonoylglycerol lipase has an agonist action for G-protein coupled receptors CB1 and CB2. MAGL also causes the incline in the concentration of specific lipids like lysophosphatidic acid, phosphatidic acid, prostaglandin E2 and sphingosine-1-phosphate derived from free fatty acids which play important role in the proliferation of cells, survival, migration, metastases, and development. In the current work, we are presenting the docking-based screening studies of various designed MAGL inhibitors by studying the different essential features of previously developed different potent inhibitors of enzyme monoacylglycerol lipase.

KEYWORDS: Inflammation; Cancer; Inhibitors; Lipase; Enzyme; Anticancer; Arachidonic acid; Monoacylglycerol Lipase.

DOI Number: 10.14704/NQ.2022.20.12.NQ77356 **NeuroQuantology2022;20(12): 3469-3491**

1. INTRODUCTION:

Monoacylglycerol lipase enzyme is a potent drug target for carcinogenic diseases, and psychiatric diseases, as well as its inhibition, has also proven to be effective in the treatment of retinal disease, anxiety, depression, pain, inflammation, and inflammation are some of the nervous system disorders (Ahamed et al., 2017; Kokona et al., 2021). As a result of MAGL's hydrolysis of 2-arachidonoylglycerol (2-AG), arachidonic acid (AA) is formed, which is a precursor to proinflammatory eicosanoids, which cause neuroinflammation and ultimately lead to neurodegenerative diseases like Alzheimer's and Parkinson's disease (Kokona et al., 2021; Korhonen et al., 2014). MAGL is also found to be an important factor in the growth of certain cancer cells, therefore the inhibitors of MAGL can be proven to be good agents in the treatment of different types of cancers (Zhu et al., 2020). MAGL has an important role in the development and continuation of free fatty acid supply to cancer cells. Overactivity of MAGL is usually seen in many aggressive tumour cells compared to nonaggressive tumorigenic cells (Poli et al., 2019). MAGL takes part in the hydrolysis of monoacylglycerol in the liver and adipose

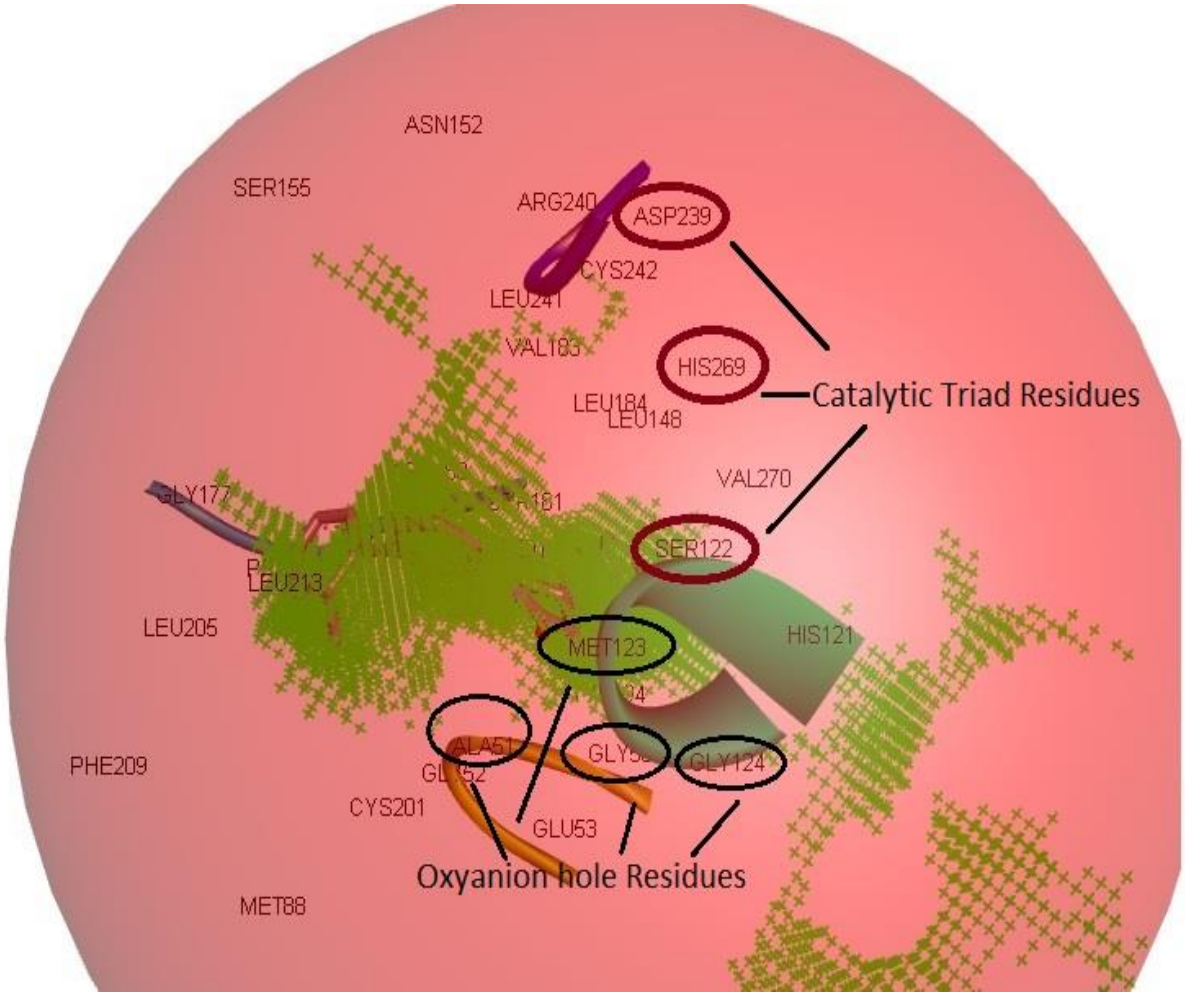

Fig. 1. Image of the binding region of 9JX containing catalytic triad residue and oxyanion hole residues by using BIOVIA Discovery Studio Visualizer 2020.

tissues, which contributes a large amount of FFA (free fatty acid) for the growth of developing tumour cells and also for the development of protumourgenic signalling factors (Poli et al., 2019; Tuccinardi et al., 2014). Monoacylglycerol lipase is a key serine hydrolase enzyme and activity is seen higher in aggressive cancer cells compared to nonaggressive cancer cells (Bononi et al., 2018; Pagano et al., 2017). MAGL is a 33 kDa hydrolase enzyme which takes part in the hydrolysis of serine and preferentially breakdown the monoacylglycerols into free fatty acids (FFA) and glycerol (Bononi et al., 2018; Tuccinardi et al., 2014). AEA and 2-AG act as a ligand and major endocannabinoids for both cannabinoid receptors. Endocannabinoids (eCB) are transported to the cytoplasm and where they get breakdown by their particular enzymes. AEA get hydrolysed by fatty acid amide hydrolase (FAAH) to Arachidonic acid (AA) and ethanolamine, where 2-AG is mainly hydrolysed by up to 85% into AA and glycerol by MAGL (Ahamed et al., 2017; Chen et al., 2019; Poli et al., 2019). Thus the inhibition of the monoacylglycerol lipase can increase the level of 2-AG, which initiates the activation of the neurotransmission system and anxiolytic, antiemetic, anti-inflammatory, neuroprotective and anti-nociceptive action can be seen in the brain (Aghazadeh Tabrizi et al., 2018; Mori et al., 2019; Zhang et al., 2019). Human MAGL consists of an alpha/ beta hydrolase fold (Cheng et al., 2018). The active site is observed in the middle of both the helices alpha and beta and it is called a catalytic triad and it is consist of Ser 122, His 269 and Asp 239 (Afzal et al., 2016; Chen et al., 2019; Cheng et al., 2018; Lauria et al., 2015; Ma et al., 2016; Scalvini et al., 2016). Another section

which contains the amphiphilic and hydrophobic properties, an extensive section of the binding pocket is called a lipophilic region of the acyl carrier binding region (ACB cavity). On attachment of 2-AG in the ACB domain (Acyl carrier binding pocket) the activation occurs of Ser122 and its rush to the carbon which contains the carbonyl group of 2-AG (Mori et al., 2019). MAGL is also composed of nucleophilic regions and contains binding loops α1 and β3, whereas it β3conatains the residues Ala51, Met123, Gly50 and Gly124, collectively referred to as oxyanion holes. (Berdan et al., 2016; Sherer & Snape, 2015). The cytoplasmic access channel (CA channel) is another name of the catalytic triad that contains polar residue to a greater extent and due to the polarity of these residues, they do interact with a 2-AG hydrophilic portion (Glycerol) and on completion of hydrolysis, release, free fatty acid and glycerol moiety (Mori et al., 2019). In this study, we performed docking studies to identify potent MAGL inhibitors as anticancer agents, based on previously developed MAGL inhibitors and their studies.

2. MATERIALS AND METHODS

2.1. DOCKING WORK

2.1.1 Computer Hardware Facılıty, Software Programs Used

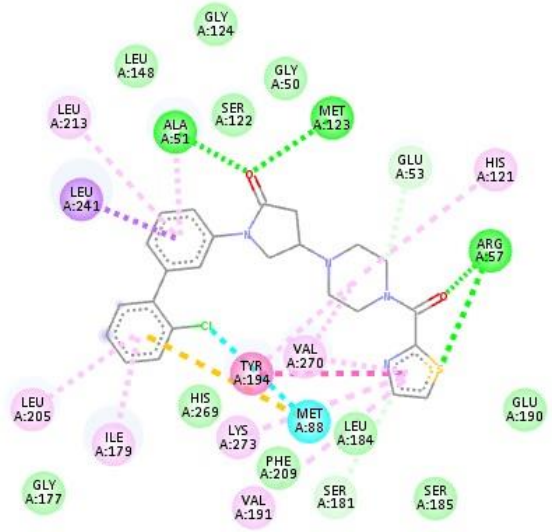

Fig. 2. 2D Image of the binding region of 9JX containing catalytic triad residue and oxyanion hole residues by using BIOVIA Discovery Studio Visualizer 2020.

The present docking studies were performed using HP laptop 64-bit apparelled with Windows 11 operating system, single language, Intel(R) Core TM i3-8130U CPU with @ 2.21 GHz processor unit, with installed random access memory (RAM) of 8GB, and SD drive of 256GB. PDB Swiss Viewer was utilized to prepare the Apo form of protein in the PDB file and the separation of the ligand as a PDB file from the original protein-ligand complex PDB file (Kaplan W, 2001). Preparation of library SDF file of 14 designed derivatives for each scaffold from 1 to 4 was performed using Open Babel software (O'Boyle et al., 2011; Swain, 2014). Preparation of reference ligand and protein for docking, conversion of compound SDF library into PDBQT, and docking of Apo form of protein and ligand libraries was performed using different wizards like Open Babel wizard and Vina wizard in PyRx virtual screening tool software (Dain et al., 123 C.E.; Dallakyan & Olson, 2015; Mai et al., 2018), Sketching, designing and preparation of ligands in 2D, SD, and another required format was performed using ACD/ChemSketch molecular structure drawing application in ACS style using structure drawing style option and OpenBabel GUI tool. Visualizations were done using BIOVIA Discovery Studio Visualizer 2020 (Tannas, 1985)(Studio 2020, 2020). Online resources used were: Protein data bank (Berman et al., 2000).

2.1.2. Monoacylglycerol lıpase enzyme binding site interaction

Monoacylglycerol lipase enzyme and ligand complex binding site interaction as well as a catalytic triad and oxyanion hole residues were visualized with the help of BIOVIA Discovery Studio Visualizer 2020. Protein PDB file 5ZUN was utilized to know the presence of catalytic triad residues and oxyanion hole residues in the protein-ligand interaction site for the identification and confirmation of the binding

region in the downloaded PDB file of a protein-ligand complex of 5ZUN.

MAGL binding site contains the catalytic triad residues Ser122, His 269 and Asp 239 (Afzal et al., 2016; Chen et al., 2019; Cheng et al., 2018; Lauria et al., 2015; Ma et al., 2016; Scalvini et al., 2016). Protein PDB file 5ZUN was downloaded from https://www.rcsb.org/ (Protein data bank) and was observed for the residues present in the ligand binding site. Catalytic triad residues Ser122, His269 and Asp239 were observed in the original ligand-protein interaction site, similarly, Gly50, Ala51, Met123 and Gly124 were also observed as oxyanion hole residues (Berdan et al., 2016; Sherer & Snape, 2015) in the ligand-protein interaction binding site.

2.1.3. procedure used in docking

A. Protein structure preparation

The PDB ID: 5ZUN X-ray crystallographic structure of Monoacylglycerol lipase along with the ligand (9JX) was chosen for this study. The PDB file format of 3 D X-ray crystallographic structure of protein and ligand was downloaded from https://www.rcsb.org/ PBD resources (protein data bank) (Berman et al., 2000) and preparation of APO form of the protein was done in the MOLPROBITY server (*Protein Science - 2017 - Williams - MolProbity More and Better Reference Data for Improved All-atom Structure Validation.Pdf*, n.d.). The preparation process of the protein involved fetching the protein molecule from the MOLPROBITY server, by uploading the PDB file of the MAGL protein molecule (PDB ID: 5ZUN). Further hydrogens were added to it and applied selected "Make Flipkin kinemages illustrating any Asn, Gln, or His flips" option to perform the tasks, which make flips to residues, analysing all the atom contacts, and geometry of the molecule. By clicking on the option software perform the job and by clicking on "download" it downloads the final protein file. The Apo form of the protein was developed using a Swiss PDB viewer, which was used further for protein preparation and finally for docking with reference ligands (9JX) and differently designed ligands.

B. Ligand Preparation

The original ligand 9JX was separated from the protein-ligand complex using a Swiss PDB viewer and saved as a different file, which was used as a reference ligand in docking. The four different scaffolds were designed in this study based on the development of previously designed compounds as MAGL inhibitors, the important features which are seen as similar in the previously developed compound were considered for the development of the new four scaffolds. From these four scaffolds, a total of 56 different derivatives were designed. 14 derivatives were designed for each scaffold and these derivatives were used as ligands are displayed in Table 1. All the structures of respective derivatives were drawn using ACD/ChemSketch molecular structure drawing application in ACS style using structure drawing style option and OpenBabel GUI software. Open Babel is also used in wizard in PyRx virtual screening tool was applied for preparation of ligands in PDBQT format for docking. The preparation process contains the insert of the SDF file of the ligand's library and minimization of all the ligands and conversion to the PDBQT format. The final stabilized structures were used for protein-ligand docking using Vina wizard in the PyRx virtual screening tool.

C. Docking Validation Studies.

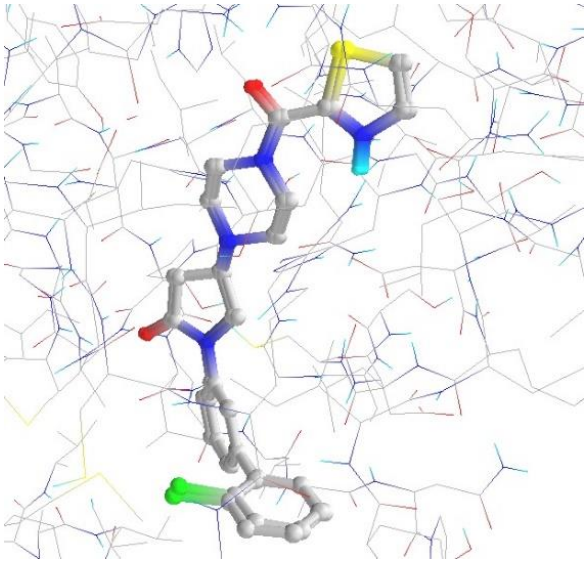

Fig. 3. Redocking pose image of validation process of protein 5ZUN with ligand 9JX.

Validation studies of the crystal structure of MAGL protein (PDB ID: 5ZUN) ligand complex with an inhibitor ligand (9JX) [(4R)-1-(2'-chloro[1,1'-biphenyl]-3-yl)-4-[4-(1,3-thiazole-2-carbonyl) piperazin-1-yl] pyrrolidin-2-one)] was performed by redocking of the separated file of ligand 9JX (co-crystallized structure of ligand) form the original PDB file and the Apo form prepared of MAGL protein file from 5ZUN into the specific binding site coordinates. The grid coordinate attributes were noted down for reference purposes.

D. Docking of Prepared Proteın and Ligand

The designed ligands docking procedures were performed by using Vina wizard in the PyRx virtual screening tool. Protein and ligand complex was subjected to the Swiss PDB viewer and the Apo form of protein and separated ligand file was generated from it, further the Apo protein file was upload to MOLPROBITY Server and the prepared protein file was download from the server and further the downloaded file was utilized for the redocking validation, as well as docking of newly designed ligands. The ligand library was generated using Open Babel software in SDF format by using smiles of all the designed ligands, further these ligand's library was minimized in Open Babel wizard in PyRx screening tool and converted all to the AutoDock PDBQT format and docking

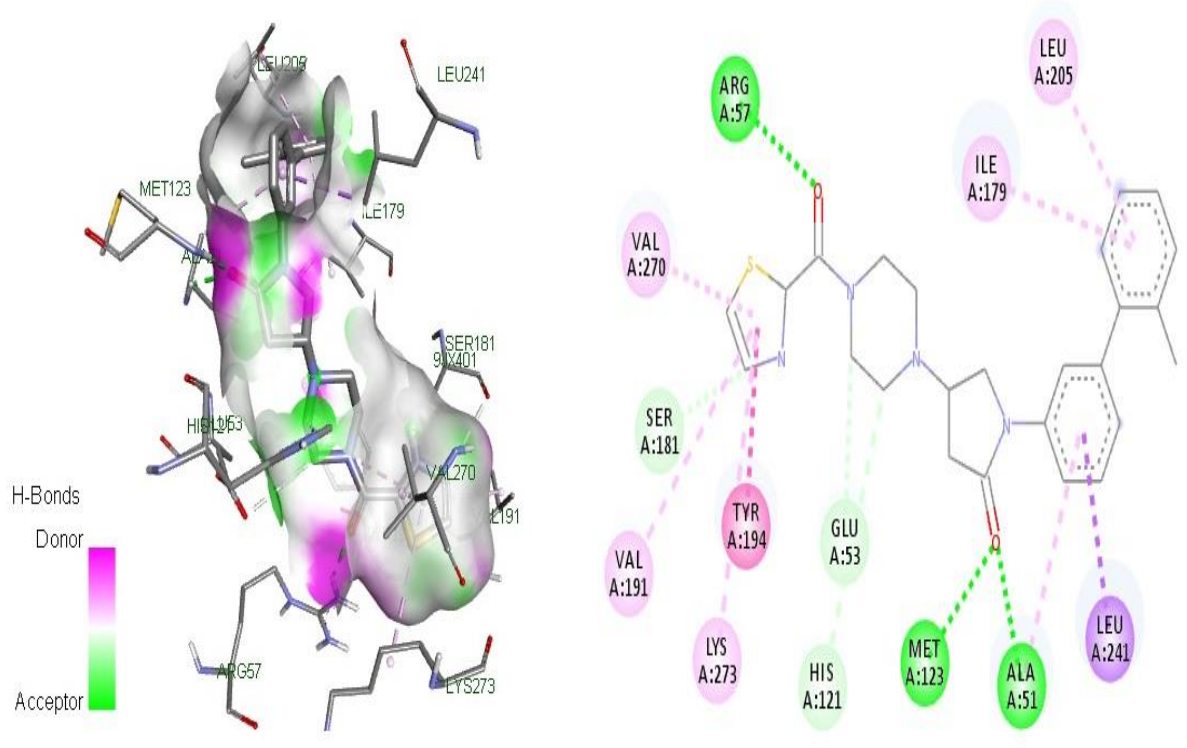

Fig. 4. 3D images and 2D images of Docking Interaction of Ligand 9JX.

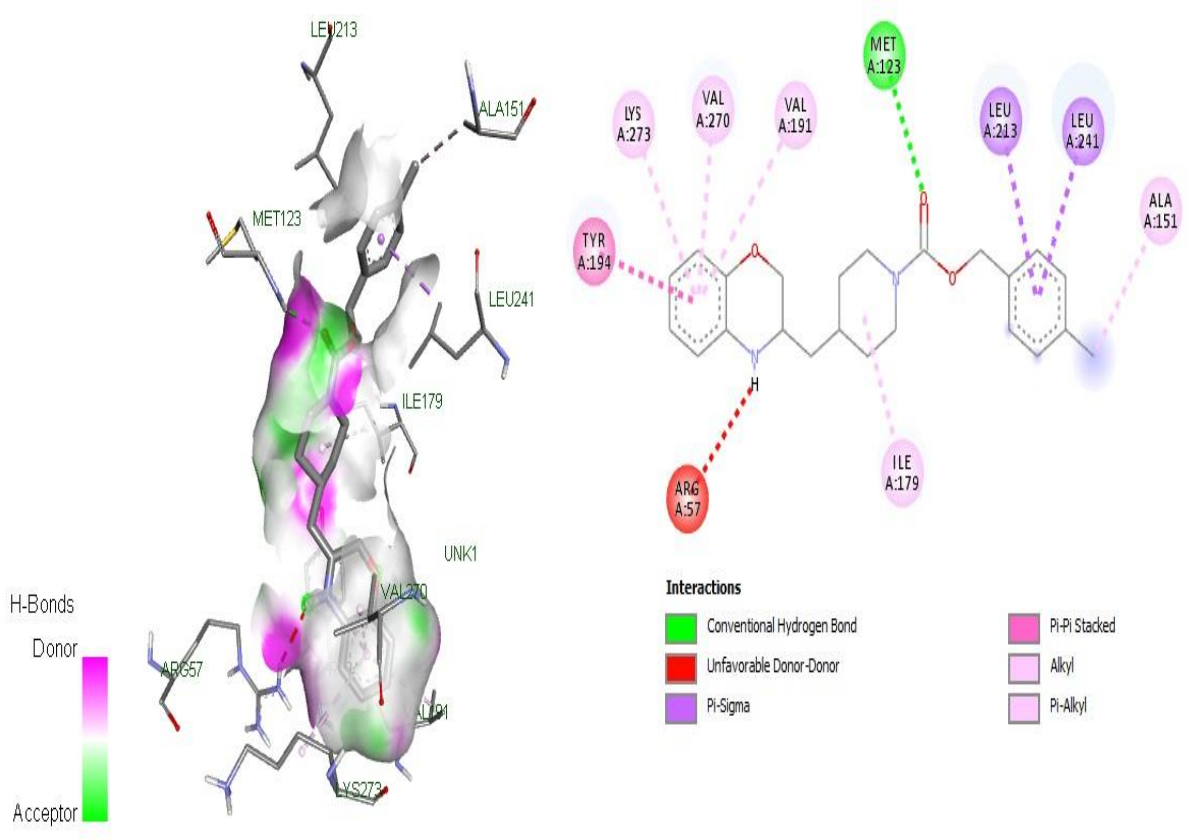

Fig. 5. 3D images and 2D images of docking interactions of Ligand S410.

procedures were involved the use of AutoDock Vina wizard in PyRx virtual screening tool. In the grid generation process, the dimensions of the grid box were used as 25x25x25 in x, y, and z directions. The attribute values coordinates were taken from binding site interactions of ligand 9JX and Protein from the original PDB file. Grid point spacing was 0.375 Å in each case. The grid Attributes were selected as X = -13.07, Y = 20.8, Z = -9.6. AutoDock Vina wizard in PyRx virtual screening tool was used to perform the molecular docking job of each ligand with prepared protein (Dain et al., 123 C.E.; Dallakyan & Olson, 2015). All the docking results were analysed of various structures were done using BIOVIA Discovery Studio Visualizer 2020 (Studio 2020, 2020).

2.2. ADME STUDIES

Adsorption, Distribution, Metabolism, and Excretion (ADME) studies are a key factor in determining whether molecules are effective and secure for further study into the possibility that the developed molecule will be employed as a significant drug in the treatment of disease. The SWISSADME web-based tool (http://www.swissadme.ch/) was utilized to

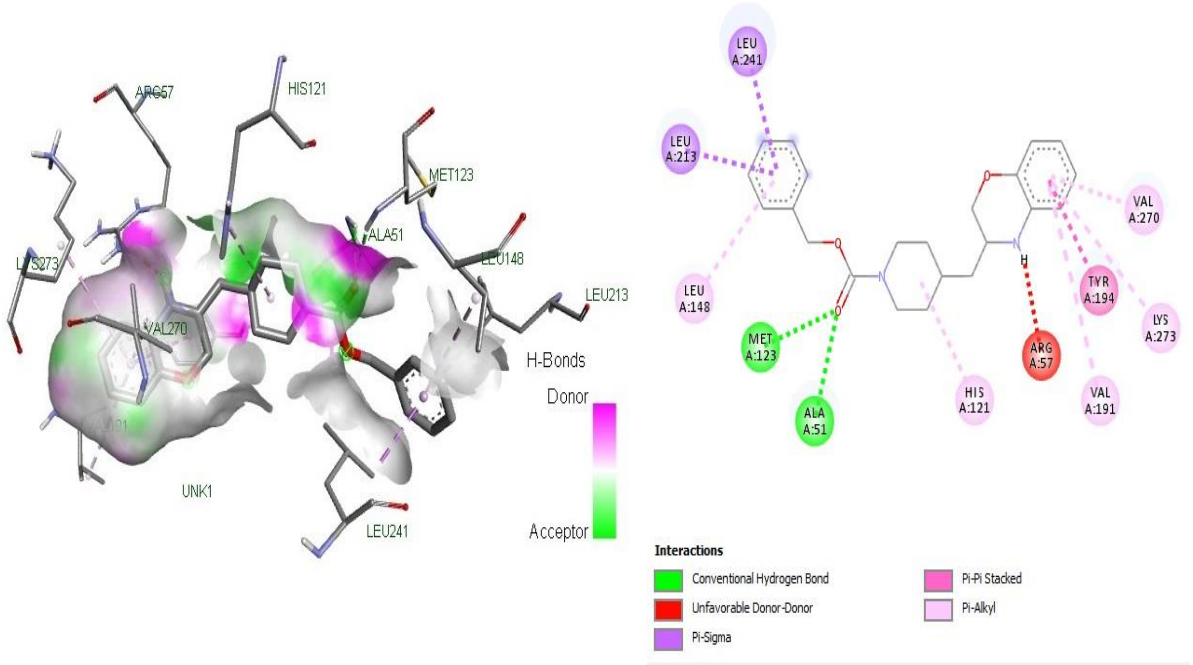

Fig. 6. 3D images and 2D images of docking interactions of Ligand S408

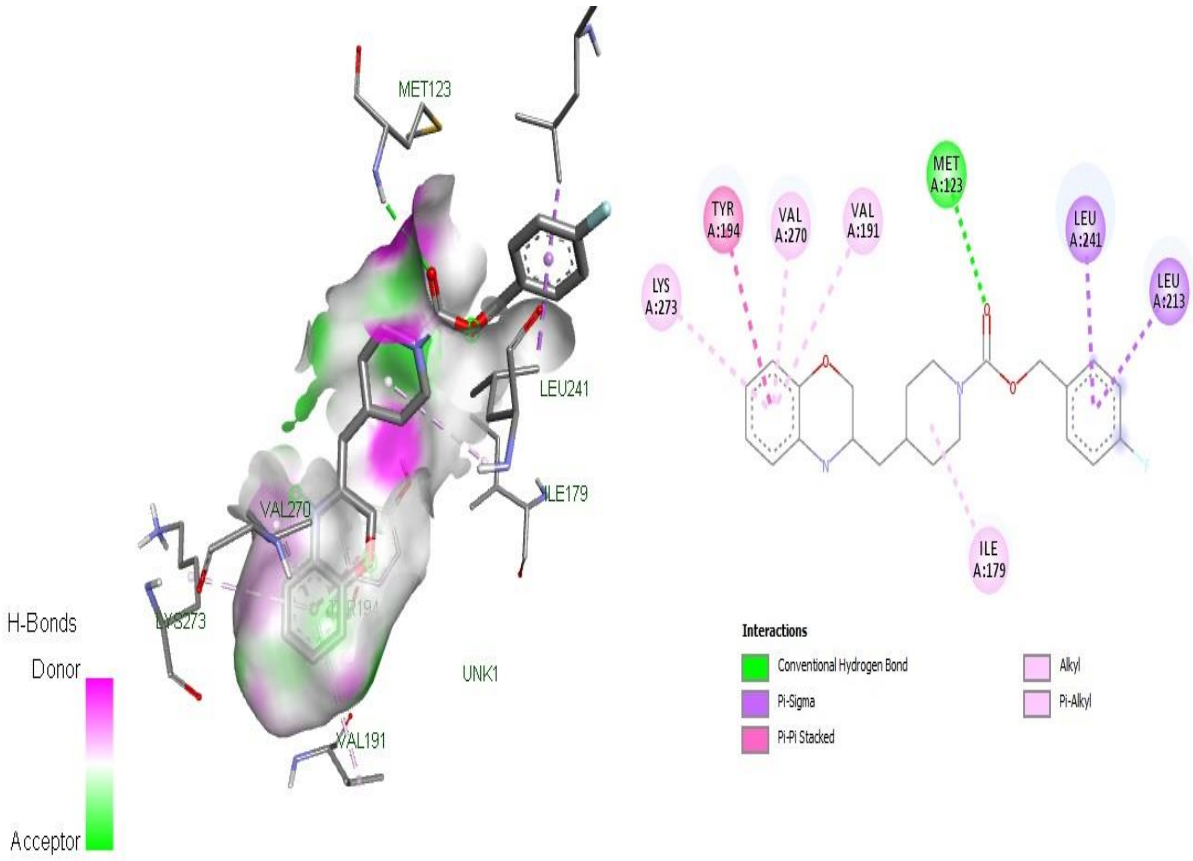

Fig. 7. 3D images and 2D images of docking interactions of Ligand S412.

identify ADME studies and predict various criteria, including lipophilicity (iLOGP, XLOGP3, WLOGP, MLOGP, SILICOS-IT), solubility in water [Log S (ESOL), Log S (Ali), Log S (SILICOS-IT)], pharmacokinetic properties [(GI absorption, BBB permeation, P-gp substrate CYP2D6, CYP3A4 CYP1A2, CYP2C19, CYP2C9, inhibitor, Log Kp), Druglikeness (Bioavailability Score Lipinski, Muegge, Ghose, Veber, Egan), Medicinal Chemistry (PAINS, Brenk, Leadlikeness, Synthetic accessibility, PAINS, Brenk, Leadlikeness, Synthetic accessibility)] (Daina et al., 2017).

SWISSADME is a web server and is developed as well as maintained by the Molecular Modelling Group of the Swiss Institute of Bioinformatics (SIB). SMILES of the different structure was submitted and results were obtained by submitting the SMILES by clicking on RUN.

2.3. TOXICITY PREDICTION

Toxicology studies were performed using the pkCSM web server database online ADMET

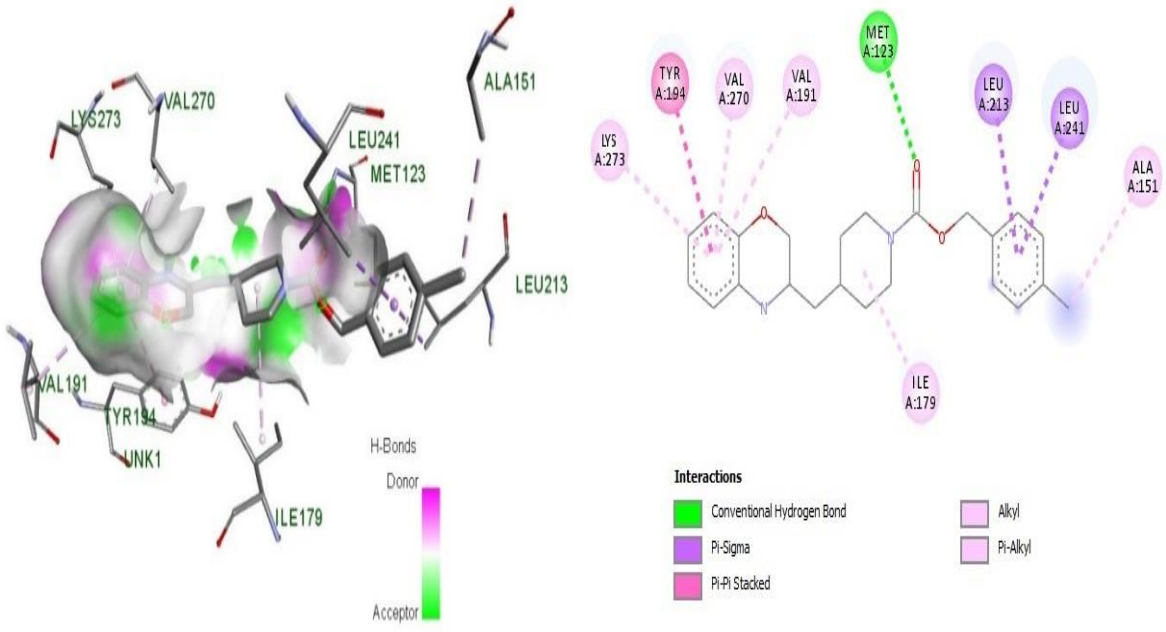

Fig. 8. 3D images and 2D images of docking interactions of Ligand S409.

prediction tool that allows to access the analysis of molecules by sketching or by uploading in SMILES format (Pires et al., 2015). Data related to toxicity includes AMES toxicity (Use to find out the carcinogenic effect of chemical), Max. tolerated dose (human), hERG I inhibitor, hERG II inhibitor (Use to find out cardiotoxicity), Oral Rat Chronic Toxicity (LOAEL), Oral Rat Acute Toxicity (LD50), Skin Sensitisation, Hepatotoxicity, T.Pyriformis toxicity, Minnow toxicity studies.

3. RESULTS AND DISCUSSION

3.1. DOCKING WORK

3.1.1. Target Binding Site Identification

Previously reported monoacylglycerol lipase blockers such as JZL184 (IC_{50} = 10 nM) and

Ly218324012 (IC_{50} = 20 nM) were found to act through the catalytic triad amino acid residues like Ser122, Asp239 and His269 and create a covalent bond formation with serine residue(Afzal et al., 2014, 2016). In the MAGL protein-ligand complex 5ZUN PDB file, the binding site of the ligand consists of the catalytic triad and the presence of residues Ser122, Asp239 and His269 were observed in the binding region of 9JX, which is displayed in Fig. 1, whereas the original ligand 9JX and original protein (5ZUN) interactions are depicted in Fig. 2. Similarly, the presence of Gly50, Ala51, Met123 and Gly124 is also observed in the binding region of 9JX, which confirms the presence of the oxyanion hole, which plays a role in the stabilization of the anionic transition state(Afzal et al., 2014). The presence of these residues in the binding region of 9JX confirms the presence of a binding pocket of MAGL enzyme, the same binding region was used with an increased grid size of 25 for XYZ dimensions for attributes X = -13.07, Y = 20.87, Z = -9.62 to cover the whole binding region.

3.1.2. Validatıon Process Results

The validation process of downloaded MAGL protein with ligand (PDB ID: 5ZUN) was performed using vina wizard in PyRx tool by redocking the ligand (9JX) with recreated Apo form of enzyme MAGL PDB file of 5ZUN. The best docking pose of the ligand was found to be superimposable on the original protein-ligand complex position. The validation studies revealed the binding energy observed for 9JX was -13.4 kcal/mol. The redocking pose is depicted in Fig. 3.

3.1.3. Docking Results

The results of the docking score of the ligands from 1 – 56 with MAGL are available in form of binding energies in negative values. The best docking score for each ligand is given in Table 2. The top ten docking score ligands are

Figure 1

Table 1. Structure of designed ligands with their codes and observed binding scores

Liagnd Code	Structure	Binding Score	Ligand Code	Structure	Binding Score
9JX	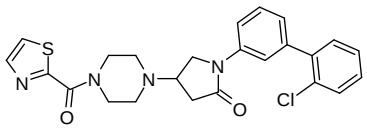	-13.4	S301	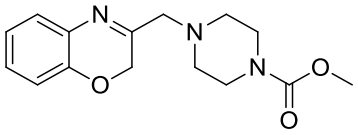	-9.9
S101	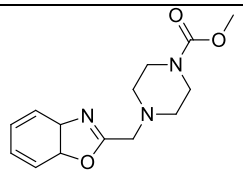	-8.6	S302	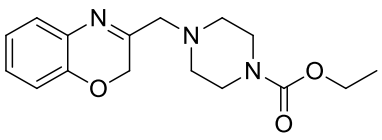	-10
S102	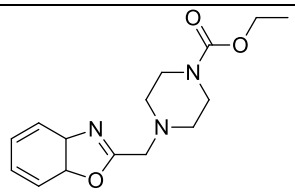	-7.7	S303	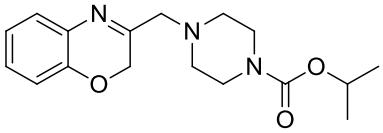	-10

S103	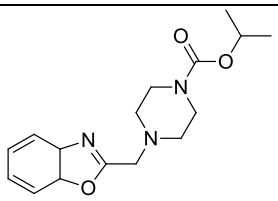	-7.8	S304	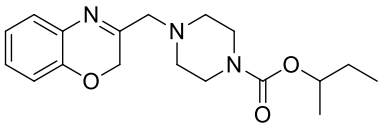	-9.7
S104	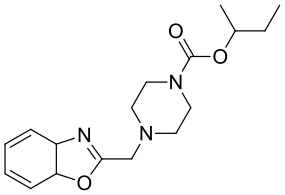	-9.9	S305	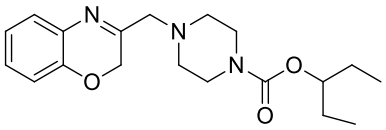	-10
S105	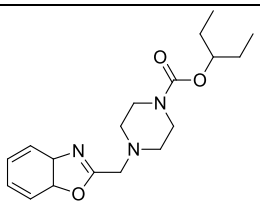	-8.1	S306	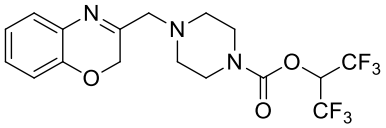	-9.6
S106	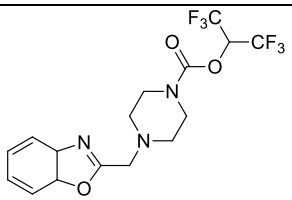	-9.8	S307	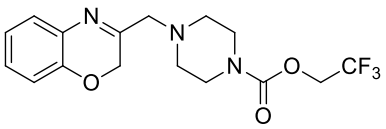	-10.5
S107	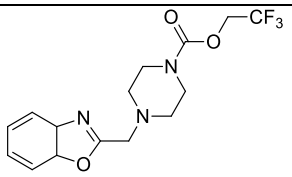	-8.7	S308	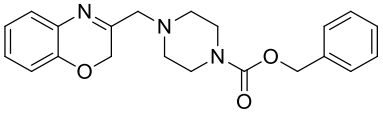	-11.5
S108	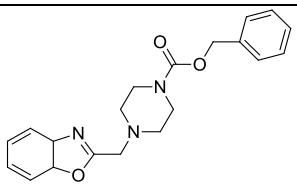	-10.6	S309	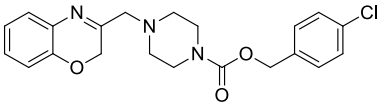	-11.2
S109	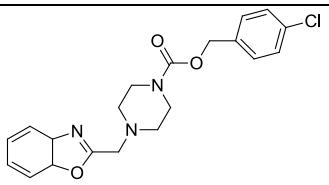	-10.7	S310	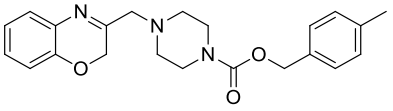	-11.4
S110	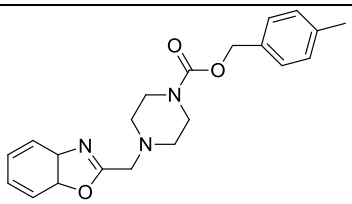	-10.9	S311	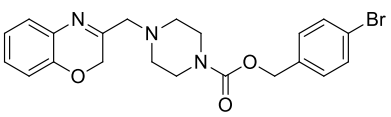	-11.4

S111	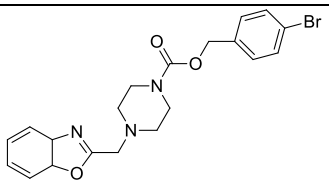	-10.6	S312	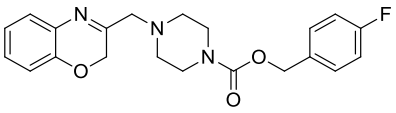	-11.4
S112	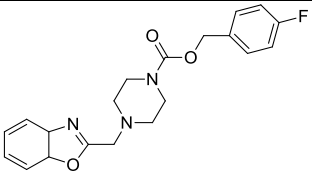	-10.3	S313	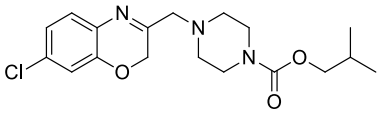	-9
S113	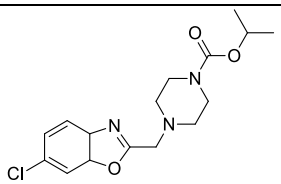	-9.3	S314	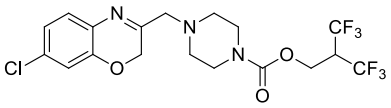	-10.2
S114	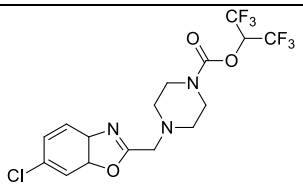	-9.4	S401	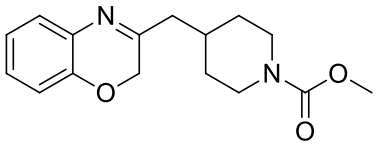	-10.2
S201	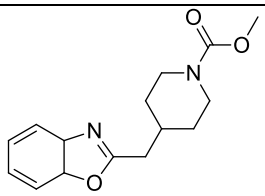	-9.7	S402	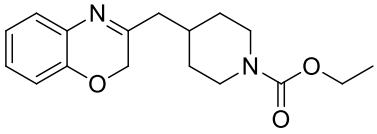	-10.3
S202	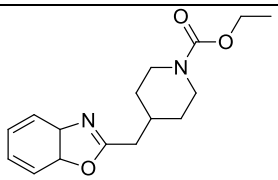	-9.6	S403	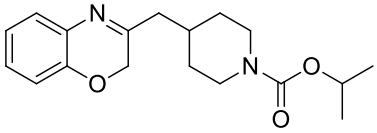	-10.5
S203	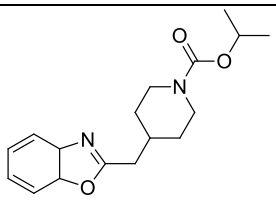	-9.3	S404	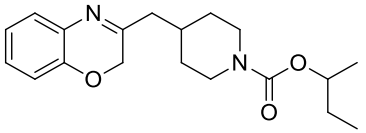	-8.8
S204	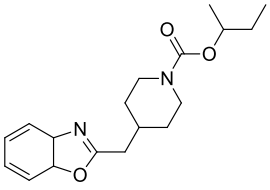	-9.3	S405	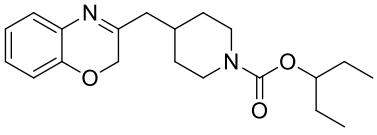	-10.4

S205	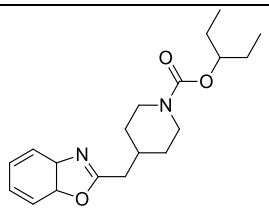	-10.1	S406	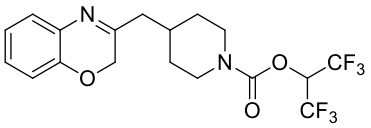	-11.5
S206	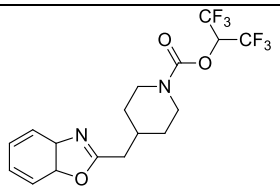	-10.1	S407	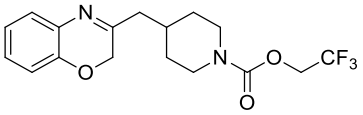	-10.8
S207	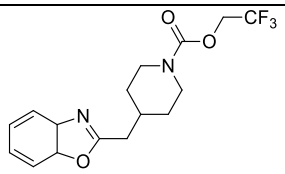	-10.3	S408	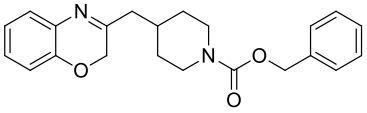	-11.6
S208	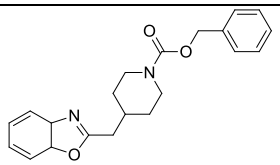	-10.6	S409	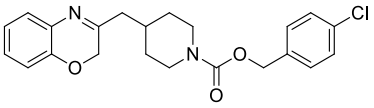	-11.9
S209	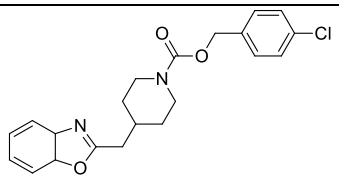	-11.1	S410	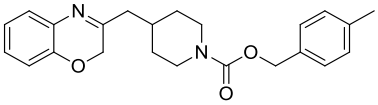	-12.3
S210	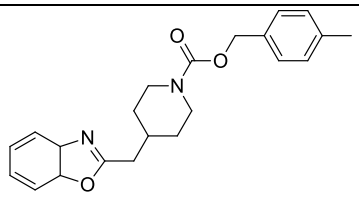	-11.4	S411	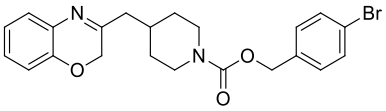	-11.7
S211	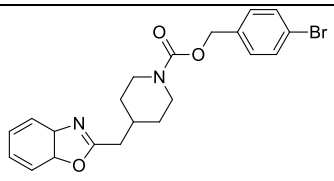	-11.4	S412	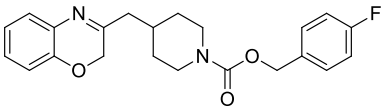	-11.9
S212	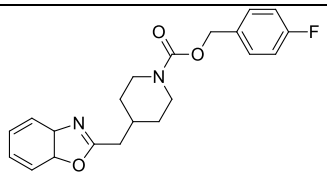	-11.2	S413	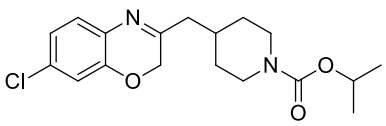	-9.7

S213	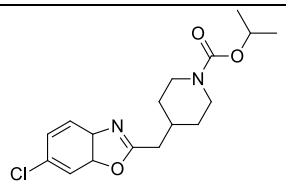	-9.7	S414	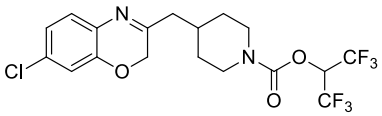	-10.6
S214	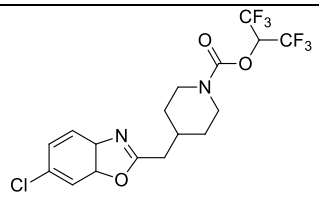	-10.5			

considered for further analysis like ADME prediction and toxicity prediction studies. The Hydrogen bond interaction and interactions with residues are given for the top ten ligands according to docking scores in Table 3. The 2D and 3D interaction images are given for these top five molecules in Figures 4 – 8.

3.2. ADME PREDİCTİON STUDİES

The best ten compounds with top docking scores compounds were subjected to the ADME investigations involving (Absorption, Distribution, Metabolism, and Excretion) by applying the online services of the SwissADME online web server tool. All ten compounds showed better GI absorption and zero violation for various drug-likeness factors Lipinski's five rules, Ghosh rule, Veber rule, Egan rule, and Muegge rule with a good 0.55 bioavailability score. All ten compounds also showed synthetic accessibility in a good range. Other criteria like LogP, Molar Refractivity, TPSA value, XLOGP3, WLOGP and MLOGP were also

Table 2. List of Top ten Ligand Docking Score (Binding energy) with PDB file 5ZUN

S. No.	Ligand No.	Docking Score
1.	Ligand 9JX	-13.4
2.	S410	-12.4
3.	S408	-11.9
4.	S412	-11.9
5.	S409	-11.8
6.	S411	-11.7
7.	S308	-11.5
8.	S210	-11.4
9.	S211	-11.4
10.	S310	-11.4
11.	S311	-11.4

Table 3. Molecular interactions of top scoring ten ligands and reference ligand

S. No.	Ligand code	No. of conventional Hydrogen bonds	H-bond forming residues	H-bond distance (Å)	Hydrophobic residues

1.	Ligand 9JX	3	ALA51, ARG57, MET123	2.09131, 2.14263, 2.19327	LEU241, TYR194, VAL191, VAL270, LYS273, ALA51, ILE179, LEU205
2.	S410	1	MET123	2.90433	LEU213, LEU241, TYR194, ALA151, ILE179, VAL191, VAL270, LYS273
3.	S408	2	ALA51, MET123	2.65195, 2.63024	LEU213, LEU241, TYR194, HIS121, VAL191, VAL270, LYS273, LEU148
4.	S412	1	MET123	2.7675	LEU213, LEU241, TYR194, ILE179, VAL191, VAL270, LYS273
5.	S409	1	MET123	2.80408	LEU213, LEU241, TYR194, ALA151, ILE179, VAL191, VAL270, LYS273
6.	S411	1	MET123	2.77965	LEU213, LEU241, TYR194, ILE179, VAL191, VAL270, LYS273
7.	S308	2	ALA51, MET123	2.63271, 2.93563	LEU213, LEU241, TYR194, VAL191, VAL270, LYS273, LEU148
8.	S210	0	-	-	LEU241, ALA151, ILE179, LEU241, HIS121, LEU148, LEU213
9.	S211	0	-	-	LEU213, LEU241, ILE179, VAL191, VAL270, LYS273, HIS121, TYR194, LEU148
10	S310	0	-	-	LEU213, LEU241, TYR194, ALA151, LEU241, VAL191, VAL270, LYS273, LEU148
11	S311	0	-	-	LEU213, LEU241, TYR194, VAL191, VAL270, LYS273

calculated. The results have been produced in Table 4.

3.3. TOXICITY STUDIES

The pkCSM server online tool was used to perform toxicity prediction studies for all the molecules according to their docking score. All

Table 4. Results of ADME Studies for the top ten ligand molecules selected on the basis top ten docking score results

Ligand	S410	S408	S412	S409	S411	S308	S210	S211	S310	S311
MR	117.64	112.67	112.63	117.68	120.37	114.67	112.96	115.7	119.64	122.37
TPSA	51.13	51.13	51.13	51.13	51.13	54.37	51.13	51.13	54.37	54.37
iLOGP	4.11	3.72	4	4.14	4.28	3.84	4.11	4.32	3.96	4.3
XLOGP3	3.89	3.52	3.62	4.15	4.21	2.69	3.49	3.82	3.05	3.38
WLOGP	3.99	3.68	4.24	4.33	4.44	1.81	3.11	3.57	2.12	2.57
MLOGP	3.16	2.95	3.32	3.43	3.53	1.91	3.3	3.67	2.13	2.51
Silicos-IT Log P	4.79	4.27	4.69	4.91	4.94	3.15	3.43	3.58	3.67	3.83
ESOL Log S	-4.56	-4.25	-4.41	-4.85	-5.16	-3.73	-4.08	-4.69	-4.04	-4.65
GI absorption	High	High	High	High	High	High	High	High	High	High
BBB permeant	Yes	Yes	Yes	Yes	Yes	Yes	Yes	Yes	Yes	Yes
log Kp (cm/s)	-5.85	-6.02	-6.06	-5.79	-6.02	-6.62	-6.06	-6.22	-6.45	-6.61
Lipinski violations	0	0	0	0	0	0	0	0	0	0
Ghose violations	0	0	0	0	0	0	0	0	0	0
Veber violations	0	0	0	0	0	0	0	0	0	0
Egan violations	0	0	0	0	0	0	0	0	0	0
Muegge violations	0	0	0	0	0	0	0	0	0	0
Bioavailability Score	0.55	0.55	0.55	0.55	0.55	0.55	0.55	0.55	0.55	0.55
PAINS alerts	0	0	0	0	0	0	0	0	0	0
Brenk alerts	0	0	0	0	0	0	0	0	0	0
Leadlikeness violations	2	2	2	2	2	1	1	2	1	1
Synthetic Accessibility	3.9	3.78	3.78	3.75	3.79	3.8	4.91	4.78	3.92	3.81

the top ten best docking score molecules were found safe for carcinogenic effect through AMES toxicity, hERG I inhibitor (cardiotoxicity) and skin sensitisation, however S410, S408, S412, S409, and S411 was also found safe hepatotoxicity profile. Compounds S203, S401, S402, and S403 were found safer for all the toxicity profiles like AMES toxicity (carcinogenic effects), hERG I inhibitor, hERG II inhibitor (cardiotoxicity), hepatotoxicity and skin sensitisation studies. The results of toxicities studies are given in Table 5.

Table 5. Results of toxicity studies performed using pkCSM web server database online ADMET prediction tool

Ligand Code	AMES toxicity	Max. tolerated dose (human)	hERG I inhibitor	hERG II inhibitor	Oral Rat Acute Toxicity (LD50)	Oral Rat Chronic Toxicity (LOAEL)	Hepatotoxicity	Skin Sensitisation
S410	No	-0.359	No	Yes	2.355	1.271	No	No
S408	No	-0.455	No	Yes	2.416	1.29	No	No
S412	No	-0.449	No	Yes	2.354	1.82	No	No
S409	No	-0.34	No	Yes	2.468	1.145	No	No
S411	No	-0.343	No	Yes	2.47	1.117	No	No
S308	No	-0.747	No	Yes	2.667	1.447	Yes	No
S210	No	-0.8	No	Yes	2.303	0.948	Yes	No
S211	No	-0.794	No	Yes	2.448	0.794	Yes	No
S310	No	-0.673	No	Yes	2.634	1.331	Yes	No
S311	No	-0.649	No	Yes	2.687	1.362	Yes	No
S203	No	-0.333	No	No	2.494	1.311	No	No
S401	No	-0.187	No	No	2.639	1.407	No	No
S402	No	-0.254	No	No	2.64	1.124	No	No
S403	No	-0.293	No	No	2.618	1.509	No	No

4. CONCLUSION

This study was performed to identify the newly designed and developed new scaffolds based on studies of previously developed compounds and their essential features for activity. By changing the features, we designed 56 ligands and, in this study, these were evaluated by docking as well as other pharmacokinetic ADME prediction online web servers tools like SwissADME and pkCSM tool for the identification of more potent and safer moiety for the treatment of cancer and other neuroinflammatory diseases as well as for other target diseases as MAGL inhibitors. The docking score results exhibited the top potent agents on basis of the top ten docking scores, which are S401, S408, S412, S409, S411, S308, S210, S211, S310, and S311. These best top ten score ligands were also evaluated for ADME prediction studies through the SwissADME online web server tool and for toxicities studies through the pkCSM online tool. All ten compounds showed better GI absorption with zero violation for all the drug-likeness criteria as well as good synthetic accessibility. Compounds S410, S408, S412, S409 and S411

also exhibited a safe profile for AMES toxicity, hERG I and hepatotoxicity and skin sensitization.

ACKNOWLEDGEMENT

None.

FUNDING

No funding is done for the present study by any source.

CONFLICT OF INTEREST

None of the authors has conflicts of interest to declare.

ETHICAL APPROVAL

This study does not involve experiments on animals or human subjects.

REFERENCES

Afzal, O., Akhtar, M. S., Kumar, S., Ali, M. R., Jaggi, M., & Bawa, S. (2016). Hit to lead optimization of a series of N-[4-(1,3-benzothiazol-2-yl)phenyl]acetamides as monoacylglycerol lipase inhibitors with potential anticancer activity. *European Journal of Medicinal Chemistry*. https://doi.org/10.1016/j.ejmech.2016.05.038

Afzal, O., Kumar, S., Kumar, R., Firoz, A., Jaggi, M., & Bawa, S. (2014). Docking based virtual screening and molecular dynamics study to identify potential monoacylglycerol lipase inhibitors. *Bioorganic and Medicinal Chemistry Letters*, *24*(16), 3986–3996. https://doi.org/10.1016/j.bmcl.2014.06.029

Aghazadeh Tabrizi, M., Baraldi, P. G., Baraldi, S., Ruggiero, E., De Stefano, L., Rizzolio, F., Di Cesare Mannelli, L., Ghelardini, C., Chicca, A., Lapillo, M., Gertsch, J., Manera, C., Macchia, M., Martinelli, A., Granchi, C., Minutolo, F., & Tuccinardi, T. (2018). Discovery of 1,5-Diphenylpyrazole-3-Carboxamide Derivatives as Potent, Reversible, and Selective Monoacylglycerol Lipase (MAGL) Inhibitors. *Journal of Medicinal Chemistry*. https://doi.org/10.1021/acs.jmedchem.7b01845

Ahamed, M., Attili, B., van Veghel, D., Ooms, M., Berben, P., Celen, S., Koole, M., Declercq, L., Savinainen, J. R., Laitinen, J. T., Verbruggen, A., & Bormans, G. (2017). Synthesis and preclinical evaluation of [11C]MA-PB-1 for in vivo imaging of brain monoacylglycerol lipase (MAGL). *European Journal of Medicinal Chemistry*. https://doi.org/10.1016/j.ejmech.2017.04.066

Berdan, C. A., Erion, K. A., Burritt, N. E., Corkey, B. E., & Deeney, J. T. (2016). Inhibition of monoacylglycerol lipase activity decreases glucose-stimulated insulin secretion in INS-1 (832/13) cells and rat islets. *PLoS ONE*, *11*(2), e0149008. https://doi.org/10.1371/journal.pone.0149008

Berman, H. M., Westbrook, J., Feng, Z., Gilliland, G., Bhat, T. N., Weissig, H., Shindyalov, I. N., & Bourne, P. E. (2000). The Protein Data Bank. *Nucleic Acids Research*, *28*(1), 235–242. https://doi.org/10.1093/NAR/28.1.235

Bononi, G., Granchi, C., Lapillo, M., Giannotti, M., Nieri, D., Fortunato, S., Boustani, M. El, Caligiuri, I., Poli, G., Carlson, K. E., Kim, S. H., Macchia, M., Martinelli, A., Rizzolio, F., Chicca, A., Katzenellenbogen, J. A., Minutolo, F., & Tuccinardi, T. (2018). Discovery of long-chain salicylketoxime derivatives as monoacylglycerol lipase (MAGL) inhibitors. *European Journal of Medicinal Chemistry*, *157*, 817–836. https://doi.org/10.1016/j.ejmech.2018.08.038

Chen, Z., Mori, W., Fu, H., Schafroth, M. A., Hatori, A., Shao, T., Zhang, G., Van, R. S., Zhang, Y., Hu, K., Fujinaga, M., Wang, L., Belov, V., Ogasawara, D., Giffenig, P., Deng, X., Rong, J., Yu, Q., Zhang, X., … Liang, S. H. (2019). Design, Synthesis, and Evaluation of 18F-Labeled Monoacylglycerol Lipase Inhibitors as Novel Positron Emission Tomography Probes. *Journal of Medicinal Chemistry*. https://doi.org/10.1021/acs.jmedchem.9

b00936

Cheng, B., Yuan, W. E., Su, J., Liu, Y., & Chen, J. (2018). Recent advances in small molecule based cancer immunotherapy. In *European Journal of Medicinal Chemistry*. https://doi.org/10.1016/j.ejmech.2018.08.028

Dain, F. A., Opo, M., Rahman, M. M., Ahammad, F., Ahmed, I., Bhuiyan, A., & Asiri, A. M. (123 C.E.). Structure based pharmacophore modeling, virtual screening, molecular docking and ADMET approaches for identification of natural anti-cancer agents targeting XIAP protein. *Scientific Reports |*, *11*, 4049. https://doi.org/10.1038/s41598-021-83626-x

Daina, A., Michielin, O., & Zoete, V. (2017). SwissADME: A free web tool to evaluate pharmacokinetics, drug-likeness and medicinal chemistry friendliness of small molecules. *Scientific Reports*, *7*(October 2016), 1–13. https://doi.org/10.1038/srep42717

Dallakyan, S., & Olson, A. (2015). Participation in global governance: Coordinating "the voices of those most affected by food insecurity." *Global Food Security Governance*, *1263*, 1–11. https://doi.org/10.1007/978-1-4939-2269-7

Kaplan W, L. T. (2001). Software review Swiss-PDB Viewer (Deep View). *Briefings in Bioinformatics*, *2*(2), 195–197.

Kokona, D., Spyridakos, D., Tzatzarakis, M., Papadogkonaki, S., Filidou, E., Arvanitidis, K. I., Kolios, G., Lamani, M., Makriyannis, A., Malamas, M. S., & Thermos, K. (2021). The endocannabinoid 2-arachidonoylglycerol and dual ABHD6/MAGL enzyme inhibitors display neuroprotective and anti-inflammatory actions in the in vivo retinal model of AMPA excitotoxicity. *Neuropharmacology*, *185*(August 2020), 108450. https://doi.org/10.1016/j.neuropharm.2021.108450

Korhonen, J., Kuusisto, A., Van Bruchem, J., Patel, J. Z., Laitinen, T., Navia-Paldanius, D., Laitinen, J. T., Savinainen, J. R., Parkkari, T., & Nevalainen, T. J. (2014). Piperazine and piperidine carboxamides and carbamates as inhibitors of fatty acid amide hydrolase (FAAH) and monoacylglycerol lipase (MAGL). *Bioorganic and Medicinal Chemistry*, *22*(23), 6694–6705. https://doi.org/10.1016/j.bmc.2014.09.012

Lauria, S., Casati, S., & Ciuffreda, P. (2015). Synthesis and characterization of a new fluorogenic substrate for monoacylglycerol lipase and application to inhibition studies. *Analytical and Bioanalytical Chemistry*, *407*(26), 1–5. https://doi.org/10.1007/s00216-015-8991-9

Ma, M., Bai, J., Ling, Y., Chang, W., Xie, G., Li, R., Wang, G., & Tao, K. (2016). Monoacylglycerol lipase inhibitor JZL184 regulates apoptosis and migration of colorectal cancer cells. *Molecular Medicine Reports*, *13*(3), 2850–2856. https://doi.org/10.3892/mmr.2016.4829

Mai, C., Nakorn, A., & Park, I. (2018). Thai Journal of Pharmaceutical Sciences (TJPS). *Thai Journal of Pharmaceutical Sciences*, *42*(supplement), 93–97. http://www.tjps.pharm.chula.ac.th/proceedings/backend/proceeding_file/24_PN_FP_Sukanya Settharaksa (102-106).pdf

Mori, W., Hatori, A., Zhang, Y., Kurihara, Y., Yamasaki, T., Xie, L., Kumata, K., Hu, K., Fujinaga, M., & Zhang, M. R. (2019). Radiosynthesis and evaluation of a novel monoacylglycerol lipase radiotracer: 1,1,1,3,3,3-hexafluoropropan-2-yl-3-(1-benzyl-1H-pyrazol-3-yl)azetidine-1-[11C]carboxylate. *Bioorganic and Medicinal Chemistry*, *27*(16), 3568–3573. https://doi.org/10.1016/j.bmc.2019.06.037

O'Boyle, N. M., Banck, M., James, C. A., Morley, C., Vandermeersch, T., & Hutchison, G. R. (2011). Open Babel. *Journal of Cheminformatics*, *3*(33), 1–14. https://jcheminf.biomedcentral.com/track/pdf/10.1186/1758-2946-3-33

Pagano, E., Borrelli, F., Orlando, P., Romano,

B., Monti, M., Morbidelli, L., Aviello, G., Imperatore, R., Capasso, R., Piscitelli, F., Buono, L., Di Marzo, V., & Izzo, A. A. (2017). Pharmacological inhibition of MAGL attenuates experimental colon carcinogenesis. *Pharmacological Research*, *119*, 227–236. https://doi.org/10.1016/j.phrs.2017.02.002

Pires, D. E. V., Blundell, T. L., & Ascher, D. B. (2015). pkCSM: Predicting small-molecule pharmacokinetic and toxicity properties using graph-based signatures. *Journal of Medicinal Chemistry*, *58*(9), 4066–4072. https://doi.org/10.1021/acs.jmedchem.5b00104

Poli, G., Lapillo, M., Jha, V., Mouawad, N., Caligiuri, I., Macchia, M., Minutolo, F., Rizzolio, F., Tuccinardi, T., & Granchi, C. (2019). Computationally driven discovery of phenyl(piperazin-1-yl)methanone derivatives as reversible monoacylglycerol lipase (MAGL) inhibitors. *Journal of Enzyme Inhibition and Medicinal Chemistry*. https://doi.org/10.1080/14756366.2019.1571271

Protein Science - 2017 - Williams - MolProbity More and better reference data for improved all-atom structure validation.pdf. (n.d.).

Scalvini, L., Vacondio, F., Bassi, M., Pala, D., Lodola, A., Rivara, S., Jung, K. M., Piomelli, D., & Mor, M. (2016). Free-energy studies reveal a possible mechanism for oxidation-dependent inhibition of MGL. *Scientific Reports*, *6*(April), 1–12. https://doi.org/10.1038/srep31046

Sherer, C., & Snape, T. J. (2015). Heterocyclic scaffolds as promising anticancer agents against tumours of the central nervous system: Exploring the scope of indole and carbazole derivatives. In *European Journal of Medicinal Chemistry* (Vol. 97, Issue 1, pp. 552–560). Elsevier Masson s.r.l. https://doi.org/10.1016/j.ejmech.2014.11.007

Studio 2020, B. D. (2020). Dassault Systems: San Diego. *CA, USA*.

Swain, C. (2014). *Open Babel Documentation*.

Tannas, L. E. (1985). System Requirements. *Flat-Panel Displays and CRTs*, 31–53. https://doi.org/10.1007/978-94-011-7062-8_2

Tuccinardi, T., Granchi, C., Rizzolio, F., Caligiuri, I., Battistello, V., Toffoli, G., Minutolo, F., Macchia, M., & Martinelli, A. (2014). Identification and characterization of a new reversible MAGL inhibitor. *Bioorganic and Medicinal Chemistry*, *22*(13), 3285–3291. https://doi.org/10.1016/j.bmc.2014.04.057

Zhang, L., Butler, C. R., Maresca, K. P., Takano, A., Nag, S., Jia, Z., Arakawa, R., Piro, J. R., Samad, T., Smith, D. L., Nason, D. M., O'Neil, S., McAllister, L., Schildknegt, K., Trapa, P., McCarthy, T. J., Villalobos, A., & Halldin, C. (2019). Identification and Development of an Irreversible Monoacylglycerol Lipase (MAGL) Positron Emission Tomography (PET) Radioligand with High Specificity. *Journal of Medicinal Chemistry*. https://doi.org/10.1021/acs.jmedchem.9b00847

Zhu, B., Connolly, P. J., Zhang, S. P., Chevalier, K. M., Milligan, C. M., Flores, C. M., & Macielag, M. J. (2020). The discovery of diazetidinyl diamides as potent and reversible inhibitors of monoacylglycerol lipase (MAGL). *Bioorganic and Medicinal Chemistry Letters*, *30*(12), 127198. https://doi.org/10.1016/j.bmcl.2020.127198